

Open Bis(triazolium) Structural Motifs as a Benchmark To Study Combined Hydrogen- and Halogen-Bonding Interactions in Oxoanion Recognition Processes

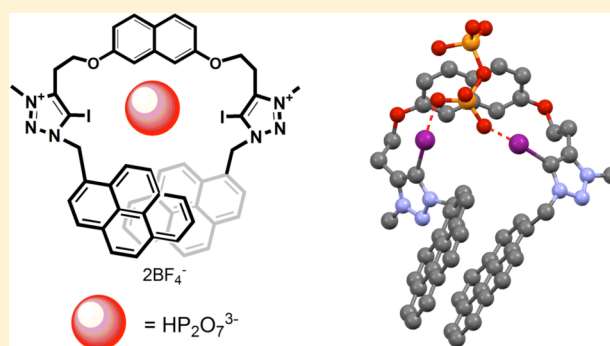
Fabiola Zapata,[†] Antonio Caballero,^{*,†} Pedro Molina,^{*,†} Ibon Alkorta,^{*,‡} and José Elguero[‡]

[†]Departamento de Química Orgánica, Universidad de Murcia, Campus de Espinardo, E-30100 Murcia, Spain

[‡]Instituto de Química Médica, Consejo Superior de Investigaciones Científicas (CSIC), Juan de la Cierva, 3, E-28006 Madrid, Spain

S Supporting Information

ABSTRACT: We have designed a series of triazolium-pyrene-based dyads to probe their potential as fluorescent chemosensors for anion recognition through combinations of hydrogen and halogen bonding. Cooperation between the two distinct non-covalent interactions leads to an unusual effect on receptor affinity, as a result of fundamental differences in the interactions of halogen and hydrogen bond donor groups with anions. Absorption, emission spectrophotometries and proton and phosphorus NMR spectroscopies indicate that the two interactions act in concert to achieve the selective binding of the hydrogen pyrophosphate anion, a conclusion supported by computational studies. Hence, as clearly demonstrated with respective halogen- and hydrogen-bonding triazolium receptors, the integration of a halogen atom into the anion receptor at the expense of one hydrogen-bonding receptor greatly influences the anion recognition affinity of the receptor. The association constant values of the halogen-bonding complexes are larger than the hydrogen-bonding counterpart. Thus, halogen bonding has been exploited for the selective fluorescent sensing of hydrogen pyrophosphate anion. Halogen bonding has been demonstrated to increase the strength of hydrogen pyrophosphate binding, as compared to the hydrogen-bonded analogue. Grimme's PBE-D functional, which adequately reproduces the pyrene stacking energies, has been successfully applied to model the affinity for anions, especially hydrogen pyrophosphate, of the new receptors.



INTRODUCTION

The field of anion recognition chemistry has expanded enormously during the past few decades due to the important roles that the anions play in chemical, biological, medical, and environmental processes.¹ Among the most promising binding strategies to target anions that have recently attracted much attention in the literature are hydrogen bonding involving a C–H donor unit, anion– π interactions, which are termed as favorable noncovalent contacts between an electron-deficient (π -acidic) aromatic system and an anion,² and halogen-bonding interactions.

Halogen bonding (XB) refers to the moderately strong, directional, noncovalent interaction of an electropositive halogen atom and a neutral or anionic Lewis base, such as N, O, S, P, or halogen functionalities and π electron donors.³ The participating partially positively charged halogen is called the halogen bond donor, whereas the Lewis base is named the halogen bond acceptor.⁴ The majority of applications of XB, including crystal engineering,⁵ chemical separations,⁶ magnetic and conductive materials,⁷ and liquid-crystalline materials,⁸ have been carried out in condensed phases. In marked contrast, with such an abundance of solid-state investigations, the recognition of anions by XB in the solution phase is only just beginning to be realized.

Incorporation of halogen bond donor groups into preorganized receptor architectures has been carried out in the context of ion-pair recognition.⁹ Multidentate perhaloarenes as halogen bond donor groups have been employed either alone¹⁰ or in combination with hydrogen bond functional groups¹¹ to achieve anion recognition in organic solvents. In this case, the low affinity of the halogen bond receptor for “hard” oxygen-based anions distinguishes them from the majority of receptors that employ hydrogen bond interactions and appears to reflect fundamental differences between the behavior of the two types of donor groups. To overcome the enthalpies of anion solvation in competitive solvents, positively charged receptors have been used. Based on this approach, anion binding properties of haloimidazolium have been reported.¹² The only reported halotriazolium is part of a rotaxane, and it has proved to be an excellent anion sensor in a competitive mixture.¹³ Importantly, the few halogen-bonding receptors designed to date, with two exceptions for dihydrogen phosphate and acetate,¹⁴ exhibit an excellent selectivity for the halide anions compared to the oxoanions.

Received: May 15, 2014

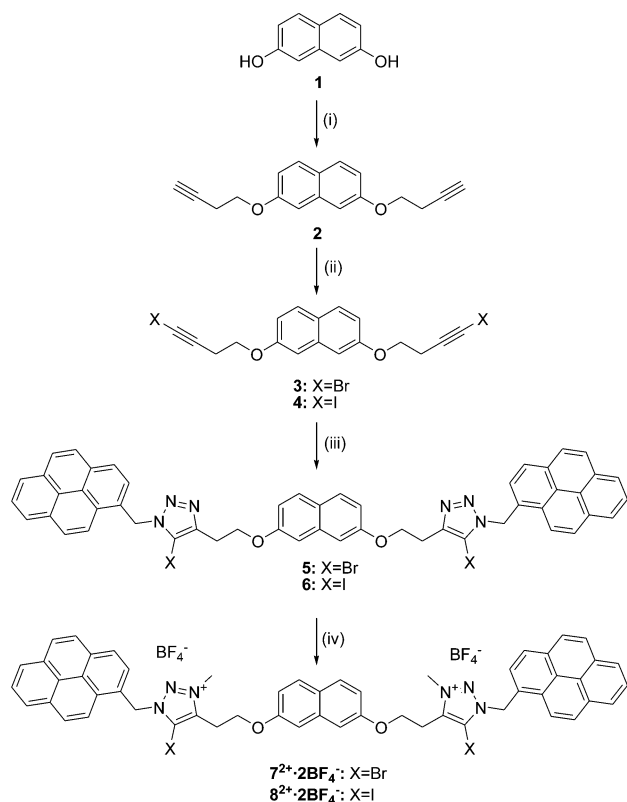
Published: July 14, 2014

With the aim of acquiring more knowledge about the behavior of halogen-bonding-based receptors in solution, we report here the synthesis and a comparative study of the anion sensing properties of a series of novel charge-assisted bidentate receptors: triazolium, halotriazolium, and a mixed bidentate receptor containing a halotriazolium unit as halogen donor and a triazolium unit as hydrogen bond unit. In addition, these kinds of receptors incorporate two end-capped photoactive pyrene rings as a fluorescent signaling unit into their host frameworks.

RESULTS AND DISCUSSION

Synthetic Strategy. Bidentate halotriazolium receptors 7^{2+} and $8^{2+} \cdot 2\text{BF}_4^-$ were prepared by a four-step procedure starting from naphthalene-2,7-diol **1** with the following sequence: (a) coupling under Mitsunobu¹⁵ conditions with but-3-yn-1-ol provided the dialkyne **2** in 50% yield; (b) bromination or iodination of **2** with NBS or NIS in the presence of catalytic amounts of AgNO_3 afforded the respective bromo- and iodoalkynes **3** (80%) and **4** (85%), respectively; (c) copper(I)-catalyzed azide–alkyne cycloaddition (CuAAC)¹⁶ reaction with 1-(azidomethyl)pyrene¹⁷ provided the corresponding bromo- and iodo-triazoles **5** and **6**, which were used without purification in the next step; and (d) methylation of **5** and **6** with trimethyloxonium tetrafluoroborate gave $7^{2+} \cdot 2\text{BF}_4^-$ and $8^{2+} \cdot 2\text{BF}_4^-$ in high yield (87–73%) (Scheme 1).

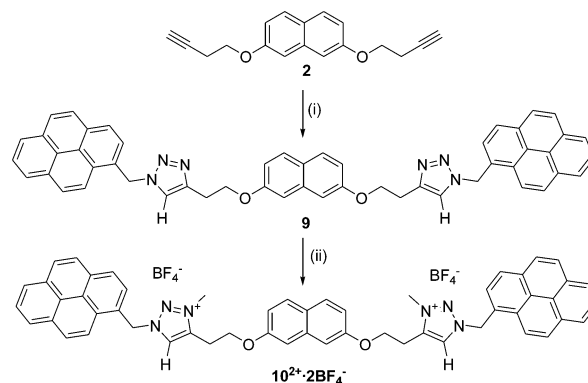
Scheme 1. Synthesis of the Bidentate Halotriazolium Receptors $7^{2+} \cdot 2\text{BF}_4^-$ and $8^{2+} \cdot 2\text{BF}_4^-$ ^a



^aReagents and conditions: (i) but-3-yn-1-ol, 0 °C, THF, PPh_3 , DEAD, 50%; (ii) NIS (X = I) or NBS (X = Br), acetone, AgNO_3 , **3**, 80%; **4**, 85%; (iii) 1-(azidomethyl)pyrene, (CuAAC), CuI (X = I) or CuBr (X = Br), THF; (iv) trimethyloxonium tetrafluoroborate, CH_2Cl_2 , $7^{2+} \cdot 2\text{BF}_4^-$, 87%; $8^{2+} \cdot 2\text{BF}_4^-$, 73%.

The analogous bidentate triazolium receptor $10^{2+} \cdot 2\text{BF}_4^-$ was synthesized following a similar synthetic procedure which involved an initial copper(I)-catalyzed azide–alkyne cycloaddition reaction between the dialkyne **2** and the 1-(azidomethyl)pyrene to give the bistriazole **9**, which underwent methylation to give the desired receptor $10^{2+} \cdot 2\text{BF}_4^-$ in 75% yield (Scheme 2).

Scheme 2. Synthesis of the Bidentate Triazolium Receptor $10^{2+} \cdot 2\text{BF}_4^-$ ^a



^aReagents and conditions: (i) 1-(azidomethyl)pyrene, TBTA, $[\text{Cu}(\text{CH}_3\text{CN})_4]\text{PF}_6$, THF; (ii) trimethyloxonium tetrafluoroborate, CH_2Cl_2 , 75%.

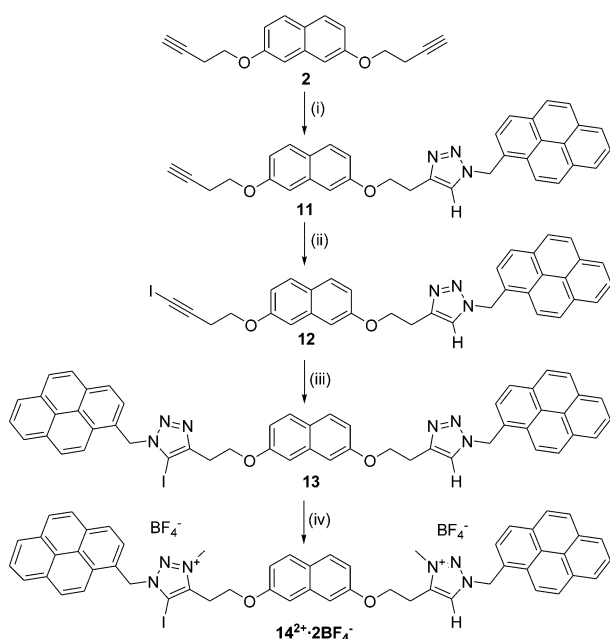
More challenging was the synthesis of the mixed bidentate receptor $14^{2+} \cdot 2\text{BF}_4^-$. Copper(I)-catalyzed azide–alkyne cycloaddition reaction between equimolar amounts of dialkyne **2** and 1-(azidomethyl)pyrene yielded the monotriazole derivative **11** in 30% yield. Iodination with NIS of **11** afforded the mono-iodinated compounds **12** in 54%. Subsequent click reaction with the same pyrenyl azide and finally methylation with trimethyloxonium tetrafluoroborate yielded the corresponding mono-iodo-bistriazolium receptor $14^{2+} \cdot 2\text{BF}_4^-$ in 75% yield (Scheme 3).

Anion Binding Studies. At first, the presence of a fluorogenic moiety such as pyrene in the prepared receptors moved us to study their anion binding affinities by observing the extent to which their fluorescence intensities were affected in the presence of various anions ($\text{HP}_2\text{O}_7^{3-}$, H_2PO_4^- , SO_4^{2-} , HSO_4^- , NO_3^- , F^- , Cl^- , Br^- , I^- , AcO^- , ClO_4^- , PF_6^- , and $\text{C}_6\text{H}_5\text{CO}_2^-$) as tetrabutylammonium salt.

The UV/vis spectra of all receptors are very similar and are characterized by an intense and broad absorption band centered at $\lambda = 343$ nm. The molar absorption coefficient ϵ is considerably higher for the non-halogenated receptor $10^{2+} \cdot 2\text{BF}_4^-$ ($\epsilon = 98\,800 \text{ M}^{-1} \cdot \text{cm}^{-1}$) than those halogenated receptors $7^{2+} \cdot 2\text{BF}_4^-$, $8^{2+} \cdot 2\text{BF}_4^-$ ($\epsilon = 88\,000$ and $50\,800 \text{ M}^{-1} \cdot \text{cm}^{-1}$, respectively) and the mixed hydrogen- and halogen-bonding receptor $14^{2+} \cdot 2\text{BF}_4^-$ ($\epsilon = 52\,400 \text{ M}^{-1} \cdot \text{cm}^{-1}$).

The addition of increasing amounts of $\text{HP}_2\text{O}_7^{3-}$ anions to a solution of the receptors $7^{2+} \cdot 2\text{BF}_4^-$, $8^{2+} \cdot 2\text{BF}_4^-$, $10^{2+} \cdot 2\text{BF}_4^-$, and $14^{2+} \cdot 2\text{BF}_4^-$ in acetone caused a small decrease in the absorption band at $\lambda = 343$ nm along with a progressive appearance of a new and weak band located at $\lambda = 349$ nm (see Supporting Information). A well-defined isosbestic point at 348 nm indicates that a neat interconversion between the noncomplexed and complexed species occurs. However, these small changes do not allow an accurate determination of the association constants.

Scheme 3. Synthesis of the Mixed Bidentate Receptor $14^{2+} \cdot 2\text{BF}_4^-$



^aReagents and conditions: (i) 1-azidomethylpyrene, TBTA, $[(\text{CH}_3\text{CN})_4]\text{PF}_6$, THF, 30%; (ii) NIS, acetone, AgNO_3 , 54%; (iii) 1-azidomethylpyrene, (CuAAC) , CuI , THF; (iv) trimethyloxonium tetrafluoroborate, CH_2Cl_2 , $14^{2+} \cdot 2\text{BF}_4^-$, 75%.

As expected, when triazolium receptors $7^{2+} \cdot 2\text{BF}_4^-$, $8^{2+} \cdot 2\text{BF}_4^-$, $10^{2+} \cdot 2\text{BF}_4^-$, and $14^{2+} \cdot 2\text{BF}_4^-$ are excited at $\lambda_{\text{ex}} = 340$ nm in acetone solution ($c = 2.5 \times 10^{-6}$ M), they exhibit the characteristic pyrene monomeric emission bands at 377, 390, and 412 nm, and a red-shifted structureless band at 473 nm, attributed to the pyrene excimer fluorescence.¹⁸ The quantum yield and the intensity ratio of the excimer to the monomer emission ($I_{\text{E}}/I_{\text{M}}$) are dependent on the structure of each receptor. The highest quantum yield corresponds to the non-halogenated receptor $10^{2+} \cdot 2\text{BF}_4^-$ ($\Phi = 0.012$); interestingly, replacement of the hydrogen atoms in the triazolium rings by halogen atoms (Br or I) induced a quenching in the fluorescence emission bands of the receptors $7^{2+} \cdot 2\text{BF}_4^-$ and $8^{2+} \cdot 2\text{BF}_4^-$. The decrease of the quantum yield depends not only on the number of halogen atoms incorporated into the receptor but also on the nature of the halogen, so that the receptor $8^{2+} \cdot 2\text{BF}_4^-$, which has two iodine atoms, exhibits the lowest quantum yield of all the studied receptors ($\Phi = 1.1 \times 10^{-3}$), which can be ascribed to an intramolecular heavy-atom effect.¹⁹ The presence of halogen atoms in the triazolium rings also inhibits the presence of the pyrene excimer emission band at $\lambda = 473$ nm. This behavior could be of particular interest in the design of turn-on fluorescent halogen-bonding-based chemosensors (Figure 1 and Table 1).

The addition of the above-mentioned set of anions to a solution of the receptors $7^{2+} \cdot 2\text{BF}_4^-$, $8^{2+} \cdot 2\text{BF}_4^-$, $10^{2+} \cdot 2\text{BF}_4^-$, and $14^{2+} \cdot 2\text{BF}_4^-$ in acetone ($c = 2.5 \times 10^{-6}$ M) demonstrates that only the addition of $\text{HP}_2\text{O}_7^{3-}$ anions promotes remarkable changes in the fluorescence spectra in all the receptors, while the addition of H_2PO_4^- and SO_4^{2-} caused small changes and the addition of HSO_4^- , NO_3^- , F^- , Cl^- , Br^- , I^- , AcO^- , ClO_4^- , PF_6^- , and $\text{C}_6\text{H}_5\text{CO}_2^-$ anions had no effect on the fluorescence spectrum even in the presence of a large excess of anions added (Figure 2).

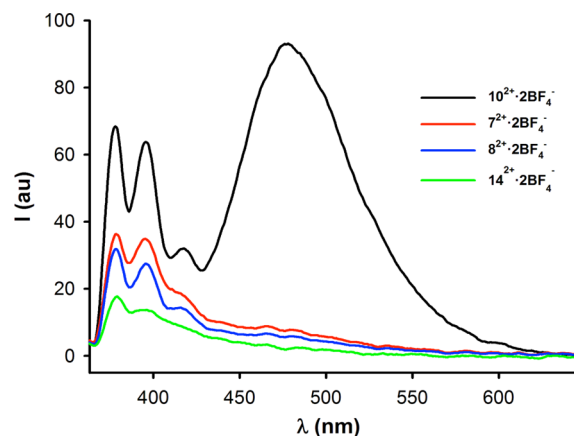


Figure 1. Fluorescence spectra of receptors $7^{2+} \cdot 2\text{BF}_4^-$, $8^{2+} \cdot 2\text{BF}_4^-$, $10^{2+} \cdot 2\text{BF}_4^-$, and $14^{2+} \cdot 2\text{BF}_4^-$ in acetone ($c = 2.5 \times 10^{-6}$ M), $\lambda_{\text{ex}} = 340$ nm.

Table 1. Characteristic Parameters of the Emission Spectra of $7^{2+} \cdot 2\text{BF}_4^-$, $8^{2+} \cdot 2\text{BF}_4^-$, $10^{2+} \cdot 2\text{BF}_4^-$, $14^{2+} \cdot 2\text{BF}_4^-$, and Their Complexes with $\text{HP}_2\text{O}_7^{3-}$ and H_2PO_4^- Anions

	Φ	$I(\lambda = 473 \text{ nm})$ (au)	$I_{\text{E}}/I_{\text{M}}$
$7^{2+} \cdot 2\text{BF}_4^-$	1.3×10^{-3}	9	0.20
$8^{2+} \cdot 2\text{BF}_4^-$	1.1×10^{-3}	6	0.18
$10^{2+} \cdot 2\text{BF}_4^-$	1.2×10^{-2}	98	1.36
$14^{2+} \cdot 2\text{BF}_4^-$	2.3×10^{-3}	3	0.12
$7^{2+} \cdot \text{HP}_2\text{O}_7^{3-}$	9.1×10^{-3}	77	11
$8^{2+} \cdot \text{HP}_2\text{O}_7^{3-}$	17.6×10^{-3}	129	21
$10^{2+} \cdot \text{HP}_2\text{O}_7^{3-}$	7×10^{-2}	656	8.62
$14^{2+} \cdot \text{HP}_2\text{O}_7^{3-}$	4.4×10^{-2}	100	3
$7^{2+} \cdot \text{H}_2\text{PO}_4^-$	4.5×10^{-2}	34	1.1
$8^{2+} \cdot \text{H}_2\text{PO}_4^-$	4.7×10^{-3}	56	1.47
$10^{2+} \cdot \text{H}_2\text{PO}_4^-$	7×10^{-2}	220	3
$14^{2+} \cdot \text{H}_2\text{PO}_4^-$	4.4×10^{-2}	48	2

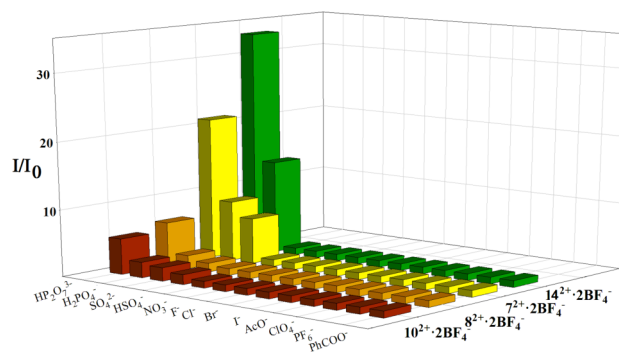


Figure 2. Graphical representation of the relative intensity of the emission band at $\lambda = 473$ nm of receptors $7^{2+} \cdot 2\text{BF}_4^-$, $8^{2+} \cdot 2\text{BF}_4^-$, $10^{2+} \cdot 2\text{BF}_4^-$, and $14^{2+} \cdot 2\text{BF}_4^-$ upon addition of 1 equiv of various anions in acetone solution at 20°C .

The addition of the $\text{HP}_2\text{O}_7^{3-}$ anions to the receptors $7^{2+} \cdot 2\text{BF}_4^-$, $8^{2+} \cdot 2\text{BF}_4^-$, and $14^{2+} \cdot 2\text{BF}_4^-$ promotes remarkable perturbations in the emission spectra, increasing the intensity of the excimer emission band at $\lambda = 473$ nm, in the ratio $I_{\text{excimer}}/I_{\text{monomer}}$ ($I_{\text{E}}/I_{\text{M}}$), and in the quantum yields. These changes were also observed in the analogous non-halogenated receptor $10^{2+} \cdot 2\text{BF}_4^-$ although to a lesser extent (Table 1). Thus, the intensity of the emission band at $\lambda = 473$ nm in the complexes was found to be 6.7–33.3 higher than those observed in the free receptors,

and the quantum yields resulted in 5.8–19-fold increase (Table 2).

Table 2. Ratio of Parameters in the Spectra Emission of Receptors $7^{2+}\cdot 2\text{BF}_4^-$, $8^{2+}\cdot 2\text{BF}_4^-$, $10^{2+}\cdot 2\text{BF}_4^-$, and $14^{2+}\cdot 2\text{BF}_4^-$ after Addition of $\text{HP}_2\text{O}_7^{3-}$ Anions

	$I_{\text{complex}}/I_{\text{receptor}}^a$	$(I_E/I_M)_{\text{complex}}/b$ $(I_E/I_M)_{\text{receptor}}$	Φ_{complex}/c Φ_{receptor}
$7^{2+}\cdot\text{HP}_2\text{O}_7^{3-}$	8.6	55	7
$8^{2+}\cdot\text{HP}_2\text{O}_7^{3-}$	21.5	116	16
$10^{2+}\cdot\text{HP}_2\text{O}_7^{3-}$	6.7	5.4	5.8
$14^{2+}\cdot\text{HP}_2\text{O}_7^{3-}$	33.3	2.5	19

^aRatio of the fluorescence intensity at $\lambda = 473$ nm between the complex and receptor. ^bRatio of the excimer and monomer emission bands (I_E/I_M) between the complex and receptor. ^cRatio of the quantum yield Φ between the complex and receptor.

The titration profile data revealed a 1:1 binding model. The association constants were obtained by fitting the respective titration data to a 1:1 host–guest binding model using the Specfit program²⁰ (Figure 3a,b).

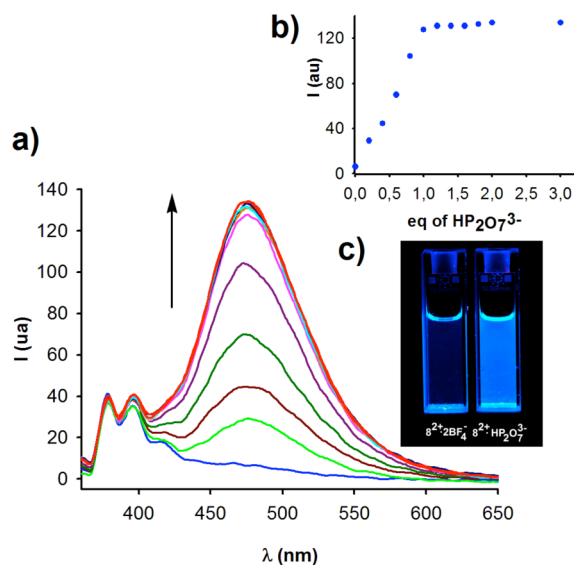


Figure 3. (a) Changes in the fluorescence spectra of receptor $8^{2+}\cdot 2\text{BF}_4^-$ (2.5×10^{-6} M) in acetone upon addition of $\text{HP}_2\text{O}_7^{3-}$ anions at 20 °C. (b) Changes of emission at $\lambda = 473$ nm of receptor $8^{2+}\cdot 2\text{BF}_4^-$ upon addition of $\text{HP}_2\text{O}_7^{3-}$. (c) Visual changes in the fluorescence of receptor $8^{2+}\cdot 2\text{BF}_4^-$ upon addition of $\text{HP}_2\text{O}_7^{3-}$ ions.

The association constants calculated for all receptors were higher than 10^6 M^{-1} , and the calculated detection limits were $1.9 \times 10^{-7} \text{ M}$ for $7^{2+}\cdot 2\text{BF}_4^-$, $2.3 \times 10^{-7} \text{ M}$ for $8^{2+}\cdot 2\text{BF}_4^-$, $1.8 \times 10^{-7} \text{ M}$ for the $10^{2+}\cdot 2\text{BF}_4^-$, and $1.6 \times 10^{-7} \text{ M}$ for $14^{2+}\cdot 2\text{BF}_4^-$. The association constant values determined for the H_2PO_4^- anion for the same receptors are smaller in magnitude than those found with $\text{HP}_2\text{O}_7^{3-}$ anions (Table 3).

The receptors $7^{2+}\cdot 2\text{BF}_4^-$, $8^{2+}\cdot 2\text{BF}_4^-$, $10^{2+}\cdot 2\text{BF}_4^-$, and $14^{2+}\cdot 2\text{BF}_4^-$ can be used as fluorescent “naked eye” chemosensor molecules for $\text{HP}_2\text{O}_7^{3-}$ anions due to the increase of the fluorescence intensity of the excimer band (Figure 3c). Among anions, hydrogen pyrophosphate ($\text{HP}_2\text{O}_7^{3-}$) is a biologically important target because it plays an important role in energy transduction in organism and controls metabolic processes by participation in enzymatic reactions.²¹ Furthermore, the

Table 3. Association Constant for Receptors $7^{2+}\cdot 2\text{BF}_4^-$, $8^{2+}\cdot 2\text{BF}_4^-$, $10^{2+}\cdot 2\text{BF}_4^-$, and $14^{2+}\cdot 2\text{BF}_4^-$ with $\text{HP}_2\text{O}_7^{3-}$ and H_2PO_4^- Anions

	$\text{HP}_2\text{O}_7^{3-} (M^{-1})$	$\text{H}_2\text{PO}_4^- (M^{-1})$
$7^{2+}\cdot 2\text{BF}_4^-$	$>10^6$	5.01×10^5
$8^{2+}\cdot 2\text{BF}_4^-$	$>10^6$	1×10^6
$10^{2+}\cdot 2\text{BF}_4^-$	$>10^6$	3.16×10^5
$14^{2+}\cdot 2\text{BF}_4^-$	$>10^6$	6.31×10^4

^aIn acetone at 20 °C.

detection of pyrophosphate has also been considered important in cancer research as telomerase (a biomarker for cancer diagnosis) activity is measured by evaluating the amount of pyrophosphate in the PCR amplification of the telomerase elongation product.²² Furthermore, the high level of pyrophosphate in synovial fluids is correlated to calcium pyrophosphate dehydrate disease (CPDD), a rheumatologic disorder.²³ Therefore, the detection and discrimination of this anion has been the main focus of the effort of several research groups.²⁴

NMR Spectroscopic Studies. In order to get additional information about the binding mode between the receptors $7^{2+}\cdot 2\text{BF}_4^-$, $8^{2+}\cdot 2\text{BF}_4^-$, $10^{2+}\cdot 2\text{BF}_4^-$, and $14^{2+}\cdot 2\text{BF}_4^-$ with $\text{HP}_2\text{O}_7^{3-}$ anions, ^1H NMR and ^{31}P NMR titration experiments were performed in order to avoid precipitation problems. NMR titration experiments were performed by adding aliquots of anion to a solution of the receptors in 9:1 $\text{CD}_3\text{CN}/\text{CD}_3\text{OD}$.

Receptors $7^{2+}\cdot 2\text{BF}_4^-$, $8^{2+}\cdot 2\text{BF}_4^-$, and $10^{2+}\cdot 2\text{BF}_4^-$ have similar ^1H NMR spectra and exhibit four sets of signals: (a) the corresponding methylene protons of the fragment $\text{O}-\text{CH}_2-\text{CH}_2-\text{triazolium}$ ring which appears as two different triplets around $\delta = 3.40$ and $\delta = 3.30$ ppm; (b) a singlet corresponding to the triazolium- CH_2 -pyrene ring; (c) the naphthalene protons which appear in the aromatic region from $\delta = 6.90$ to $\delta = 7.60$ ppm; and (d) the pyrene protons which appear as a complex signal from $\delta = 8.00$ to $\delta = 8.40$ ppm. In addition, the non-halogenated receptor $10^{2+}\cdot 2\text{BF}_4^-$, shown as a singlet, was attributed to the proton of the triazolium ring which appears within in the pyrene region. As expected in the mixed bidentate receptor $14^{2+}\cdot 2\text{BF}_4^-$, the different nature of the substituent in the triazolium rings induces a splitting not only of the two arms of the receptor but also of the central naphthalene linker.

Addition of $\text{HP}_2\text{O}_7^{3-}$ anions to a solution of the halogenated receptors $7^{2+}\cdot 2\text{BF}_4^-$ and $8^{2+}\cdot 2\text{BF}_4^-$ promotes similar changes in the chemical shift in the ^1H NMR spectra, although these changes are significantly greater in magnitude for the bis-iodotriazolium receptor $8^{2+}\cdot 2\text{BF}_4^-$ than for the bis-bromotriazolium receptor $7^{2+}\cdot 2\text{BF}_4^-$.

The addition of increasing amounts of $\text{HP}_2\text{O}_7^{3-}$ anions to a solution of the receptor $8^{2+}\cdot 2\text{BF}_4^-$ in 9:1 $\text{CD}_3\text{CN}/\text{CD}_3\text{OD}$ induced significant downfield shifts in the naphthalene H_c proton and in the methylene $\text{CH}_2-\text{O}-$ (H_e) protons, $\Delta\delta = 0.19$ and $\Delta\delta = 0.16$ ppm, respectively, whereas the CH_2 -pyrene protons (H_a) and the remaining naphthalene protons (H_b and H_d) were upfield shifted, $\Delta\delta = -0.17$, $\Delta\delta = -0.07$, and $\Delta\delta = -0.13$ ppm, respectively. Importantly, a remarkable upfield shift ($\Delta\delta \sim -0.12$ ppm) was also observed in all the pyrene protons, which is indicative of aromatic $\pi-\pi$ interactions between both pyrene rings of the receptor, and is in good agreement with the presence of the excimer emission band observed after addition of $\text{HP}_2\text{O}_7^{3-}$ anions in the fluorescence experiments (Figure 4a).

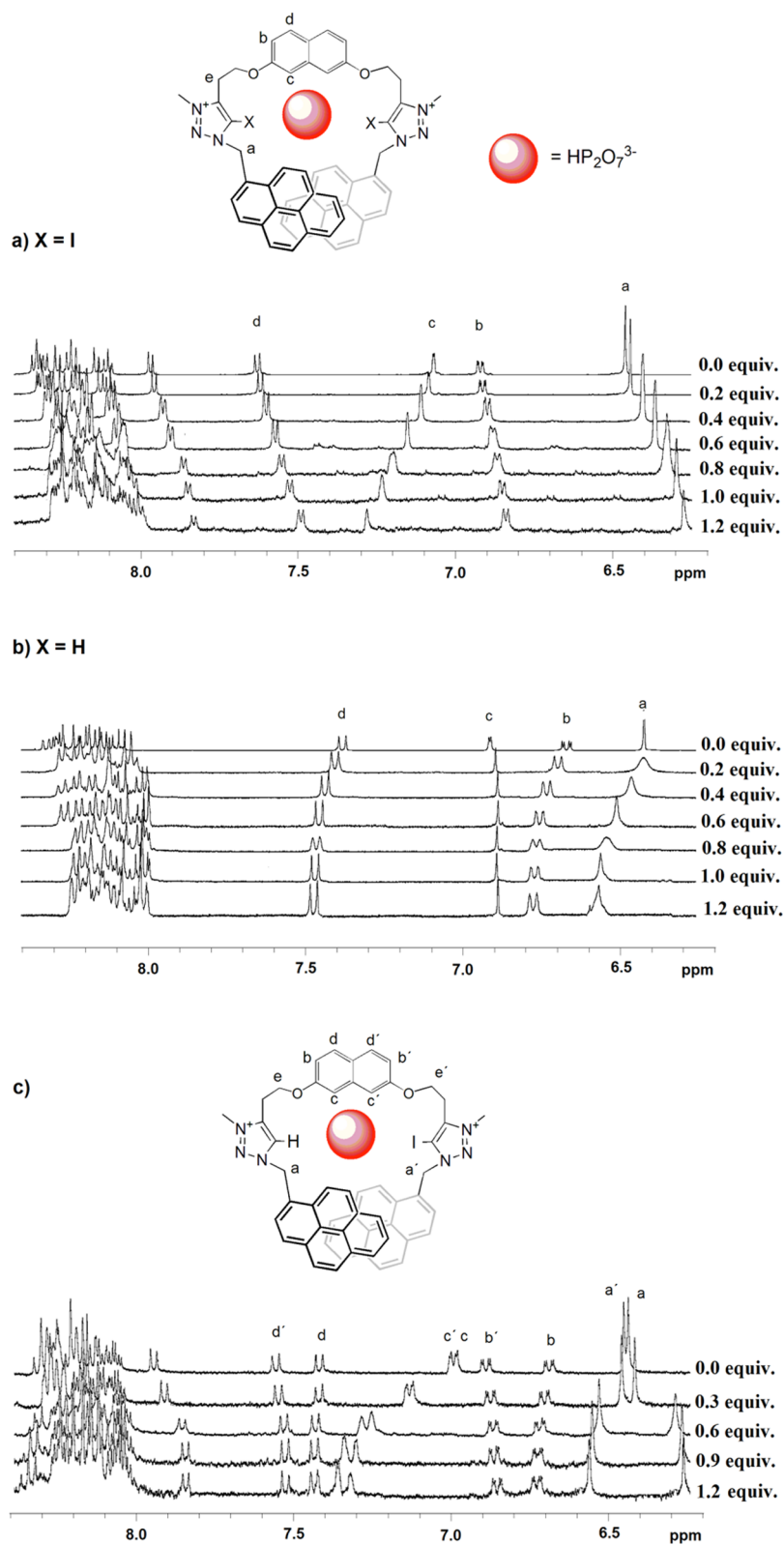


Figure 4. ^1H NMR spectral changes observed in receptors (a) $8^{2+} \cdot 2\text{BF}_4^-$, (b) $10^{2+} \cdot 2\text{BF}_4^-$, and (c) $14^{2+} \cdot 2\text{BF}_4^-$ ($c = 2.5 \times 10^{-3} \text{ M}$ in $9:1 \text{ CH}_3\text{CN}/\text{CD}_3\text{OD}$) during the addition of up to 1.2 equiv of $\text{HP}_2\text{O}_7^{3-}$ anions.

The addition of $\text{HP}_2\text{O}_7^{3-}$ anions to the non-halogenated receptor $10^{2+} \cdot 2\text{BF}_4^-$ showed a different behavior than that observed with the halogen-bonding receptors $7^{2+} \cdot 2\text{BF}_4^-$ and $8^{2+} \cdot 2\text{BF}_4^-$. Thus, addition of $\text{HP}_2\text{O}_7^{3-}$ to $10^{2+} \cdot 2\text{BF}_4^-$ promotes the downfield shift of the CH_2 -pyrene H_a protons ($\Delta\delta = 0.15$) and

the naphthalene protons H_b ($\Delta\delta = 0.12$) and H_d ($\Delta\delta = 0.10$), while the H_c proton was not practically affected. On the contrary, it was noted that the upfield shift during the course of the titration in the methylene CH_2 -O- protons (H_e) ($\Delta\delta = 0.35$) and in the pyrene protons ($\Delta\delta \sim -0.12 \text{ ppm}$) was the same as

those observed for the receptors $7^{2+} \cdot 2\text{BF}_4^-$ and $8^{2+} \cdot 2\text{BF}_4^-$ (Figure 4b).

The chemical shifts observed in the mixed XB and HB receptor $14^{2+} \cdot 2\text{BF}_4^-$ after the addition of $\text{HP}_2\text{O}_7^{3-}$ anions are a combination of those described above for the XB receptors $7^{2+} \cdot 2\text{BF}_4^-$ and $8^{2+} \cdot 2\text{BF}_4^-$ and the HB receptor $10^{2+} \cdot 2\text{BF}_4^-$, with the only exception being the H_c protons. Thus, the closest proton to the iodotriazolium binding site H_a showed an upfield of $\Delta\delta = -0.18$ ppm similar to that observed for the XB receptors $7^{2+} \cdot 2\text{BF}_4^-$ and $8^{2+} \cdot 2\text{BF}_4^-$ while the H_a proton, nearest to the HB triazolium binding site, showed a downfield shift by $\Delta\delta = 0.1$ ppm as it was found in the HB receptor $10^{2+} \cdot 2\text{BF}_4^-$. Likewise, H_b and H_d protons were upfield shifted $\Delta\delta = -0.03$ ppm, whereas H_b and H_d protons were downfield shifted by $\Delta\delta = 0.03$ ppm. In contrast H_c and H_e protons underwent a remarkable downfield shift by $\Delta\delta = 0.32$ ppm, similar to those observed only in the XB receptors $7^{2+} \cdot 2\text{BF}_4^-$ and $8^{2+} \cdot 2\text{BF}_4^-$ (Figure 4c).

Addition of a large excess of HSO_4^- , NO_3^- , F^- , Cl^- , Br^- , I^- , AcO^- , ClO_4^- , PF_6^- , $\text{C}_6\text{H}_5\text{CO}_2^-$ and also H_2PO_4^- and SO_4^{2-} ions to a solution in the same solvent of the receptors $7^{2+} \cdot 2\text{BF}_4^-$, $8^{2+} \cdot 2\text{BF}_4^-$, $10^{2+} \cdot 2\text{BF}_4^-$, and $14^{2+} \cdot 2\text{BF}_4^-$ caused no changes in the ^1H NMR spectra of the receptors.

The chemical shifts observed in the ^{31}P NMR spectrum (see Supporting Information) of the $\text{HP}_2\text{O}_7^{3-}$ anion after the addition of 1 equiv of receptors $7^{2+} \cdot 2\text{BF}_4^-$ and $8^{2+} \cdot 2\text{BF}_4^-$, $\Delta\delta = -1.81$ and $\Delta\delta = -1.76$, respectively, are considerably higher than those observed for the receptor $10^{2+} \cdot 2\text{BF}_4^-$ ($\Delta\delta = -1.20$), while the mixed receptor $14^{2+} \cdot 2\text{BF}_4^-$ showed an intermediate chemical shift value ($\Delta\delta = -1.55$) almost the arithmetic mean between the iodate receptor and the non-halogenated one (Table 4).

Table 4. ^{31}P NMR Chemical Shifts of $\text{HP}_2\text{O}_7^{3-}$ and Complexes with $7^{2+} \cdot 2\text{BF}_4^-$, $8^{2+} \cdot 2\text{BF}_4^-$, $10^{2+} \cdot 2\text{BF}_4^-$, and $14^{2+} \cdot 2\text{BF}_4^-$ Receptors

	^{31}P (ppm) ^a
$\text{HP}_2\text{O}_7^{3-}$	-6.29
$7^{2+} \cdot 2\text{BF}_4^-$	-8.10 ($\Delta\delta = -1.81$)
$8^{2+} \cdot 2\text{BF}_4^-$	-8.05 ($\Delta\delta = -1.76$)
$10^{2+} \cdot 2\text{BF}_4^-$	-7.49 ($\Delta\delta = -1.20$)
$14^{2+} \cdot 2\text{BF}_4^-$	-7.84 ($\Delta\delta = -1.55$)

^aIn $\text{CD}_3\text{CN}/\text{CD}_3\text{OD}$ (9:1, v/v) at 20 °C.

Following an identical procedure to that reported in a previous paper,²⁵ the association constants were obtained by monitoring the chemical shift of the naphthalene protons H_c during addition of the $\text{HP}_2\text{O}_7^{3-}$ anion to the receptors (Figure 5). Job plot analysis of the titration data revealed a 1:1 receptor to anion binding stoichiometry (see Supporting Information). The association constants were obtained by fitting the titration data to a 1:1 host–guest binding model using the WinEQNMR program²⁶ and are reported in Table 5.

Theoretical Modeling. In view of the above-reported results, we decided to carry out theoretical calculations. Due to the size of the systems (all the dicationic receptors have 106 atoms), we decided to use the ADF program²⁷ using COSMO (conductor-like screening model) to model the solvent (acetone).²⁸ To select the functional and the basis set, we start by studying the pyrene dimer because this is the essential feature of the receptors. There is no experimental value, but it was estimated by a single-point MP2/6-31G calculation on the crystal structure to be $54.8 \text{ kJ}\cdot\text{mol}^{-1}$ for the slip-parallel structure.²⁹ Grimme calculated at the DFT-D-BLYP/QZV-

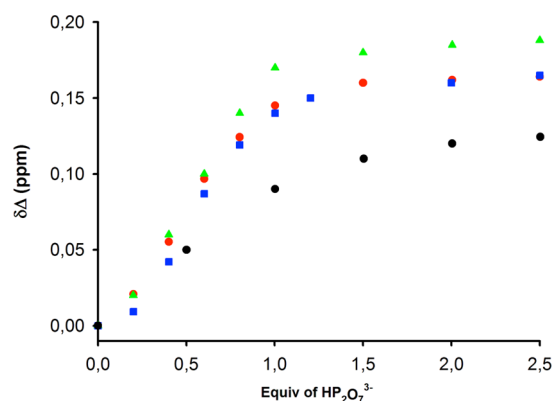


Figure 5. Titration curves by ^1H NMR for receptors $7^{2+} \cdot 2\text{BF}_4^-$ (red), $8^{2+} \cdot 2\text{BF}_4^-$ (green), $10^{2+} \cdot 2\text{BF}_4^-$ (blue), and $14^{2+} \cdot 2\text{BF}_4^-$ (black), $c = 2.5 \times 10^{-3} \text{ M}$ in 9:1 $\text{CH}_3\text{CN}/\text{CD}_3\text{OD}$ during the addition of up to 2.5 equiv of $\text{HP}_2\text{O}_7^{3-}$ anions.

Table 5. Association Constants for Receptors $7^{2+} \cdot 2\text{BF}_4^-$, $8^{2+} \cdot 2\text{BF}_4^-$, $10^{2+} \cdot 2\text{BF}_4^-$, and $14^{2+} \cdot 2\text{BF}_4^-$ with $\text{HP}_2\text{O}_7^{3-}$ Anions Calculated by ^1H NMR

receptor	K_a^a (M^{-1})
$7^{2+} \cdot 2\text{BF}_4^-$	3032 ± 270
$8^{2+} \cdot 2\text{BF}_4^-$	9838 ± 500
$10^{2+} \cdot 2\text{BF}_4^-$	1883 ± 163
$14^{2+} \cdot 2\text{BF}_4^-$	1734 ± 162

^aIn $\text{CD}_3\text{CN}/\text{CD}_3\text{OD}$ (9:1, v/v) at 20 °C.

(2df,2pd) level provided a value of $47.5 \text{ kJ}\cdot\text{mol}^{-1}$.³⁰ We tried several functionals and basis sets, and the best result ($42.9 \text{ kJ}\cdot\text{mol}^{-1}$) was obtained with the PBE-D with a dzp basis set (Slater-type basis set double- ζ + 1 polarization function).^{31,32}

We then calculate for the three homoreceptors (H–H, 10^{2+} ; Br–Br, 7^{2+} , and I–I, 8^{2+}) two conformations, the “extended” and the “tweezer” or folded one (Figure 6).

The optimized conformations of the two halogen bonding receptors 7^{2+} and 8^{2+} show different binding mode with $\text{HP}_2\text{O}_7^{3-}$ regarding to the hydrogen bonding receptor 10^{2+} and the mixed 14^{2+} . In the first case (7^{2+} and 8^{2+}) the $\text{HP}_2\text{O}_7^{3-}$ is bound to the receptors by the cooperative action of the two halotriazolium units with the two negative oxygen atoms located in one phosphorus atom of the $\text{HP}_2\text{O}_7^{3-}$, while the recognition of $\text{HP}_2\text{O}_7^{3-}$ by the receptors 10^{2+} and 14^{2+} take place by the binding of two negative oxygen atoms of the two different phosphorus atoms of $\text{HP}_2\text{O}_7^{3-}$ (Figure 7).

We have represented schematically in Figure 8 the main geometrical parameters of the complexes of Figure 7.

The C–H \cdots O $^-$ bonds belong to the category of Gilli’s charge-assisted hydrogen bonds (CAHB)³³ and more specifically to the double-charge-assisted H-bonds (\pm)-CAHB,³⁴ composed between a triazolium cation and an oxygen anion, explaining the very short H \cdots O distances (mean 1.88 Å, shortest 1.72 Å). The same happens with the halogen bonds that have very short values, C–Br \cdots O $^-$ (mean 2.53 Å, shortest 2.48 Å) and C–I \cdots O $^-$ (mean 2.59 Å, shortest 2.40 Å).³⁵ In all cases, the OH groups of the phosphates (see Supporting Information) and pyrophosphates interact with the naphthalene ring. Note that the angle of the central atom of the anion has values in the 90° zone that vary in the order $\text{I} < \text{Br} < \text{H}$; this is the normal result when the vertex is I^- or Br^- .^{9b,12b,d}

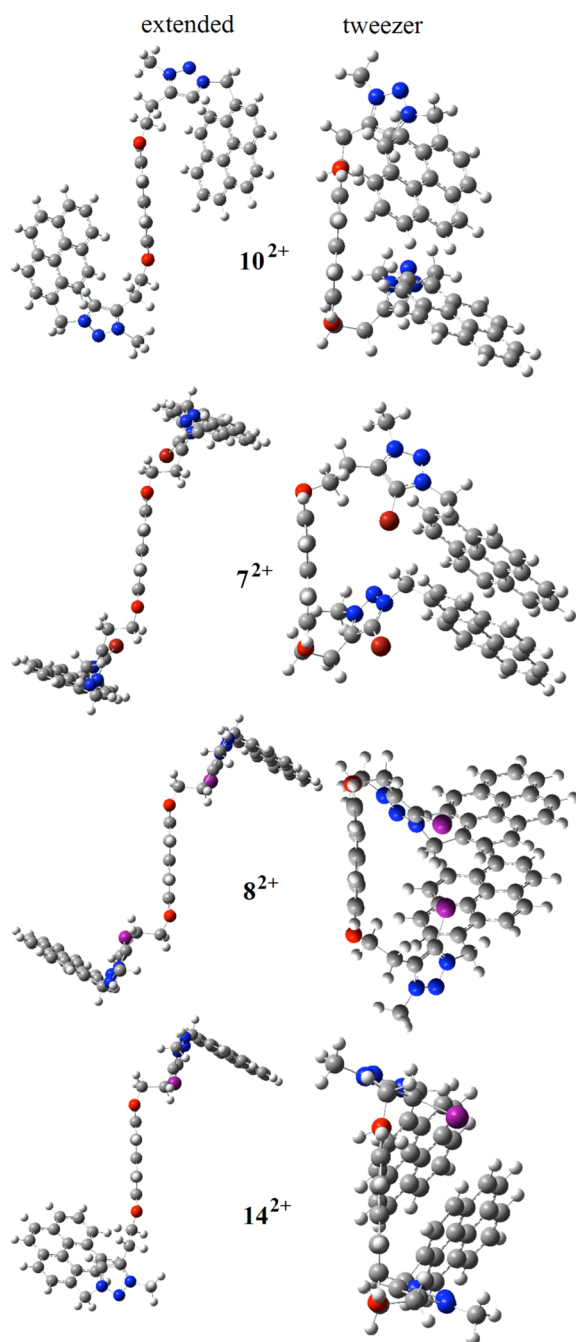


Figure 6. Two conformations of the four receptors. In all cases, the folded structures are more stable than the extended ones; differences in energy ($\text{kJ}\cdot\text{mol}^{-1}$): 10^{2+} , 46.2; 7^{2+} , 10.3; 8^{2+} , 2.1; and 14^{2+} , 16.1 $\text{kJ}\cdot\text{mol}^{-1}$.

The calculated interaction energies correspond to the difference between the complex and the sum of the host plus the guest, all of them considering the solvent as defined by the continuum models, in our case COSMO/acetone.

We have collected a series of association constants in M^{-1} determined by fluorescence in acetone (Table 3, 20 °C) and by ^1H NMR in $\text{CD}_3\text{CN}/\text{CD}_3\text{OD}$ (9:1, v/v) (Table 5, 25 °C), and from these values, we have calculated the standard Gibbs free energies ($\Delta G^\circ = -RT \ln K_a$) reported in Table 6. We have used $T = 300 \text{ K}$ in both cases.

The data of Table 6 lead to the following conclusions: (i) On average, the E_i values corresponding to the sulfate are not

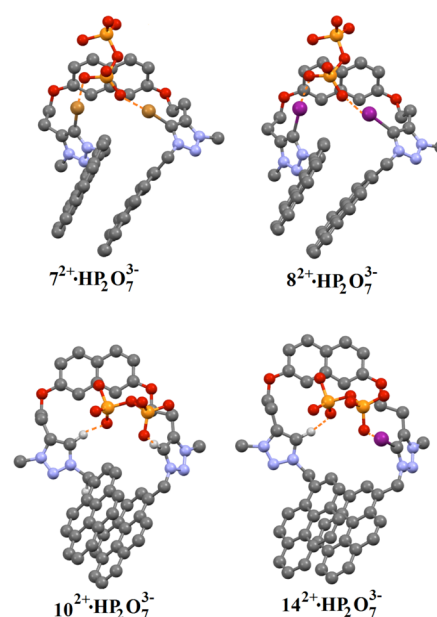


Figure 7. Conformations of the three homoreceptors (tweezer conformation) 7^{2+} , 8^{2+} and 10^{2+} with $\text{HP}_2\text{O}_7^{3-}$ anions, and the heteroreceptor 14^{2+} with $\text{HP}_2\text{O}_7^{3-}$. Hydrogen removed for clarity.

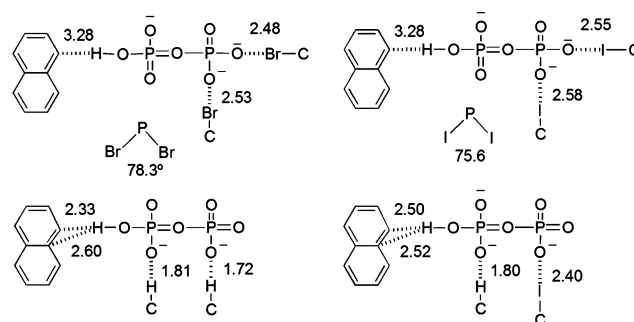


Figure 8. Schematic representation of the main interactions: distances in angstroms and angles in degrees.

Table 6. Standard Gibbs Free Energies, ΔG° ($T = 300 \text{ K}$), and Interaction Energies, E_i (Both in $\text{kJ}\cdot\text{mol}^{-1}$)

receptor	anion	method		E_i calcd
		NMR $\text{CD}_3\text{CN}/\text{CD}_3\text{OD}$ (9:1, v/v)	fluorescence (acetone)	
7^{2+}	H_2PO_4^-		-33.1	-41.8
	SO_4^{2-}			-47.1
	$\text{HP}_2\text{O}_7^{3-}$	-20.0	-43.1	-110.6
8^{2+}	H_2PO_4^-		-34.5	-47.4
	SO_4^{2-}			-67.4
	$\text{HP}_2\text{O}_7^{3-}$	-22.9	-45.7	-115.1
10^{2+}	H_2PO_4^-		-31.6	-30.3
	SO_4^{2-}			-49.4
	$\text{HP}_2\text{O}_7^{3-}$	-18.8	-43.6	-83.7
14^{2+}	H_2PO_4^-		-27.6	
	$\text{HP}_2\text{O}_7^{3-}$	-18.6	-38.3	-99.7

correlated to the other two, but the values corresponding to the hydrogen pyrophosphate are, on average, 2.6 times greater than those of the dihydrogen phosphate. (ii) Both experimental methods are correlated; the ΔG values obtained by NMR are, on average, half those obtained by fluorescence. (iii) Between E_i and

$\Delta G^\circ_{\text{fluorescence}}$, there is an equation of the form $E_i = (144 \pm 44) + (5.7 \pm 1.1)\Delta G^\circ_{\text{fluorescence}}$, $n = 7$, $R^2 = 0.83$. (iv) The worse values are $\Delta G^\circ_{\text{fluorescence}}$ of $10^{2+}/\text{HP}_2\text{O}_7^{3-}$ (measured -43.6 , fitted -40.5) and $14^{2+}/\text{HP}_2\text{O}_7^{3-}$ (measured -38.3 , fitted -41.5 $\text{kJ}\cdot\text{mol}^{-1}$).

Thus, we have two observations. First, the values of K_a determined by fluorescence (in acetone) are a little over 10 000 times greater than those determined by NMR in the 9:1 $\text{CD}_3\text{CN}/\text{CD}_3\text{OD}$ mixture (this corresponds to about 23 $\text{kJ}\cdot\text{mol}^{-1}$); then, why are the calculated interaction energies for the hydrogen pyrophosphate anion about twice those determined by fluorescence.

The first thing to take into account is related to the change of solvent: acetone for fluorescence and methanol (actually, a mixture, but 10% methanol will dominate over acetonitrile) for NMR. Association constants are very sensitive to the nature of the solvent, especially protic versus nonprotic. Several authors have pointed out that the K_a value showed considerable variation as a function of solvent identity including those involving halogen bonds;^{9b} others reported that hydrogen-bonding solvents are detrimental to the formation of halogen bonds, although the effect is hard to interpret.^{12c,36}

It has been reported that the equilibrium constants determined for association of tetrabutylammonium bromide changes from 285 in acetone to 3 in methanol (ratio: 95).³⁷ It has also been described that in the complex between [18]crown-6 and potassium isocyanate the association constant K_a increases by a factor $>10^4$ on going from water to propylene carbonate.³⁸ In solvent, effects for neutral/neutral host–guest complexes are reported to cover a range of ΔG° of 34 $\text{kJ}\cdot\text{mol}^{-1}$.³⁹

The second one is related to the fact that experimental values are free energies and calculated ones are related to enthalpies. Using the mean values of Table 6, we obtain $E_i = \Delta H^\circ = -75.5$ and $\Delta G^\circ_{\text{fluorescence}} = -38.6$ $\text{kJ}\cdot\text{mol}^{-1}$, thus $T\Delta S^\circ = 36.9$ $\text{kJ}\cdot\text{mol}^{-1}$. Water values for cyclophane/1,4-disubstituted benzenes in water have been reported to be, for instance, $\Delta G^\circ = -25$, $\Delta H^\circ = -40$, and $T\Delta S^\circ = 15$ $\text{kJ}\cdot\text{mol}^{-1}$.⁴⁰ Closer to our subject are the values found^{12c} for a halogen bond donor with halides NBu_4X , for instance, for imidazolium/ $\text{C}^+\text{I}^-\cdots\text{Br}^-\cdots\text{I}^+\text{C}/\text{imidazolium}$, $\Delta G^\circ = -32.8$, $\Delta H^\circ = -16.2$, and $T\Delta S^\circ = 16.6$ $\text{kJ}\cdot\text{mol}^{-1}$, almost exactly proportional but 2.3 times lower than our values.

CONCLUSION

The synthesis of a new family of XB halotriazolium receptors has been achieved where a naphthalene spacer group is decorated with two arms containing as binding site bromo-, iodo-, and even unsubstituted triazolium motifs, end-capped with a photoactive pyrene ring. Our synthetic methodology allows the preparation of receptors equipped with two different arms bearing both halogen and hydrogen bond donor triazolium rings to probe their potential as turn-on fluorescent chemosensors for oxoanion recognition in solution through combinations of hydrogen and halogen bonding. Several types of evidence, including the nature of the anion-induced ^1H and ^{31}P NMR spectroscopic changes, small perturbation of the absorption spectra, and the most important remarkable perturbation of the fluorescence of the receptor in the presence of the oxoanion hydrogen pyrophosphate, indicate that the two interactions occur simultaneously. The mixed halogen- and hydrogen-bonding receptor $14^{2+}\cdot 2\text{BF}_4^-$ has an association constant for $\text{HP}_2\text{O}_7^{3-}$ anions of $K_a = 1734 \pm 162$ M^{-1} ; the substitution of the triazolium (hydrogen bonding) for iodotriazolium (halogen bonding) to get the bis-iodotriazolium receptor $8^{2+}\cdot 2\text{BF}_4^-$ causes an increase in the

association constant of 5.5-fold with regard to that observed for the mixed halogen- and hydrogen-bonding receptor $14^{2+}\cdot 2\text{BF}_4^-$. Moreover, the association constant of the receptor $7^{2+}\cdot 2\text{BF}_4^-$, which has two bromotriazolium units, has an association constant of $K_a = 3032 \pm 270$ for $\text{HP}_2\text{O}_7^{3-}$ anions, which is almost twice that calculated for the mixed receptor $14^{2+}\cdot 2\text{BF}_4^-$. Consequently, the integration of a halogen atom into the anion receptor at the expense of one hydrogen-bonding receptor $14^{2+}\cdot 2\text{BF}_4^-$ greatly influences the anion recognition affinity of the receptor. The association constant values of the halogen-bonding complexes are larger than the hydrogen-bonding counterpart; in other words, halogen bonding increases the strength of hydrogen pyrophosphate binding, as compared to the hydrogen-bonded analogue. From the perspective of the anion recognition, halogen bonding has been exploited for the first time in the selective fluorescent sensing of the hydrogen pyrophosphate anion biomarker in solution, which represents one rare example of the recognition of oxoanion by a halogen-bonding interaction. Additionally, the incorporation of halogen atoms in fluorescent chemosensors has proved to be an important tool in the design of turn-on fluorescent receptors because the halogen atoms induce the fluorescence quenching in the free receptors. Theoretical calculations yield consistent results that are like a steel frame that sustain the whole building, giving confidence to our experimental results.

EXPERIMENTAL SECTION

General Comments. All reactions were carried out under N_2 and using solvents which were dried according to routine procedures. Melting points were determined on hot-plate melting point apparatus and are uncorrected. Column chromatography was run with silica gel (60 A C.C. 70–200 μm , sds) as the stationary phase with HPLC grade solvent. NMR spectra were recorded on 200, 300, and 400 MHz apparatus. The following abbreviations for stating the multiplicity of the signals in the NMR spectra were used: s (singlet), d (doublet), dd (double doublet), t (triplet), m (multiplet). Chemical shifts refer to signals of tetramethylsilane in the case of ^1H and ^{13}C spectra. UV–vis and fluorescence spectra were carried out in the solvents and concentrations stated in the text and in the corresponding figure captions, using a dissolution cell with 10 mm path length, and they were recorded with the spectra background corrected before and after sequential additions of different aliquots of anions. Mass spectrometry was recorded on an HPLC-MS TOF instrument using positive ionization. Quantum yield values were measured with respect to anthracene as standard ($\Phi = 0.27 \pm 0.01$) using the equation $\Phi_x/\Phi_s = (S_x/S_s)[(1 - 10^{-A_x})/(1 - 10^{-A_s})](n_s^2/n_x^2)$, where x and s indicate the unknown and standard solution, respectively, F is the quantum yield, S is the area under the emission curve, A is the absorbance at the excitation wavelength, and n is the refractive index. Mass spectrometry was recorded on an HPLC-MS TOF instrument using positive ionization.

2,7-Bis(but-3-ynyloxy)naphthalene 2. To a solution of naphthalene-2,7-diol (0.5 g, 3.13 mmol), but-3-yn-1-ol (0.44 g, 6.26 mmol), and PPh_3 (1.63 g, 6.26 mmol) in 100 mL of dry THF (100 mL) at 0 $^\circ\text{C}$ was added dropwise 1.03 mL (6.26 mmol) of diethyl azodicarboxylate (DEAD). Then the resulting solution was stirred for 16 h. After that, the solvent was concentrated to dryness and the resultant residue was purified by column chromatography using 8:0.5 $\text{CH}_2\text{Cl}_2/\text{EtOH}$ as eluent to give the product as a white solid (0.41 g, 50%): mp 105–106 $^\circ\text{C}$; ^1H NMR (300 MHz, CDCl_3) δ (ppm) 7.66 (2H, d, $J = 12$ Hz), 7.00–7.05 (4H, m), 4.21 (4H, t, $J = 9$ Hz), 2.75 (4H, td, $J = 9$ Hz, $J = 3$ Hz), 2.07 (2H, t, $J = 3$ Hz); ^{13}C NMR (75.5 MHz, CD_2Cl_2) δ (ppm) 157.0, 135.8, 129.1, 125.2, 116.2, 106.2, 86.1, 69.5, 66.0, 19.4; MS (ESI) m/z calcd for $\text{C}_{18}\text{H}_{16}\text{O}_2$ [$\text{M} + \text{H}$] $^+$ 265.12, found 265.13. Anal. Calcd for $\text{C}_{18}\text{H}_{16}\text{O}_2$: C, 81.79; H, 6.10. Found: C, 81.61; H, 6.08.

2,7-Bis(4-bromobut-3-ynyloxy)naphthalene 3. To a solution of the alkyne 2 (0.2 g, 0.76 mmol) in acetone (20 mL) were added *N*-bromosuccinimide (0.27 g, 0.15 mmol) and catalytic amount of silver

nitrate. The reaction mixture was stirred for 2 h at room temperature in the dark under N_2 , after which a yellow suspension was formed. All volatile components were removed under reduced pressure to give a yellow oil, which was purified by silica gel column chromatography hexane/AcOEt 7:3 to give an off-white solid (0.26 g, 80%): mp 107–108 °C; 1H NMR (300 MHz, $CDCl_3$) δ (ppm) 7.66 (2H, d, J = 8 Hz), 7.03–6.99 (4H, m), 4.19 (4H, t, J = 6 Hz), 2.76 (4H, t, J = 6 Hz); ^{13}C NMR (75.5 MHz, $CDCl_3$) δ (ppm) 156.9, 135.7, 129.2, 124.6, 116.3, 106.3, 69.9, 65.6, 40.1, 20.7; MS (ESI) m/z calcd for $C_{18}H_{14}Br_2O_2$ [$M + 1$] $^+$ 420.94, found 420.94. Anal. Calcd for $C_{18}H_{14}Br_2O_2$: C, 51.22; H, 3.34. Found: C, 51.37; H, 3.26.

2,7-Bis(4-iodobut-3-ynyloxy)naphthalene 4. To a solution of the alkyne **2** (0.5 g, 1.89 mmol) in acetone (20 mL) were added *N*-iodosuccinimide (0.85 g, 3.79 mmol) and catalytic amount of silver nitrate. The reaction mixture was stirred for 2 h at room temperature in the dark under N_2 , after which a yellow suspension was formed. All volatile components were removed under reduced pressure to give a yellow oil, which was purified by silica gel column chromatography hexane/AcOEt 7:3 to give an off-white solid (0.82 g, 85%): mp 108–109 °C; 1H NMR (300 MHz, $CDCl_3$) δ (ppm) 7.65 (2H, d, J = 8 Hz), 7.03–6.97 (4H, m), 4.19 (4H, t, J = 6 Hz), 2.91 (4H, t, J = 6 Hz); ^{13}C NMR (75.5 MHz, $CDCl_3$) δ (ppm) 156.8, 135.7, 129.2, 124.6, 116.3, 106.2, 69.9, 65.6, 40.1, 20.5; MS (ESI) m/z calcd for $C_{18}H_{14}I_2O_2$ [$M + 1$] $^+$ 516.91, found 516.91. Anal. Calcd for $C_{18}H_{14}I_2O_2$: C, 41.89; H, 2.73. Found: C, 42.01; H, 2.71.

2,7-Bis[(5-bromo-1-methyl-(pyren-1-yl)-1H-1,2,3-triazol-4-yl)-ethoxy]naphthalene 5. Copper bromide (0.102 g, 0.71 mmol) and $Cu(AcO)_2$ (0.129 g, 0.71 mmol) were stirred in dry THF (10 mL) for 20 min. The resultant solution was added to a solution of bromoalkyne **3** (0.150 g, 0.36 mmol) and 1-(azidomethyl)pyrene (0.183 g, 0.71 mmol), and the reaction mixture was stirred in the dark for 16 h at 50 °C before being quenched with 10% ammonium hydroxide solution (2 mL). Volatile components were removed under reduced pressure, and the resulting solid was filtered and washed with MeOH (3 \times 50 mL) to give the crude product **5** (0.11 g, 32%). Due to the extreme insolubility, the bis-bromotriazole **5** was only characterized by MS (ESI) and was used in the following step without further purification: MS (ESI) m/z calcd for $C_{52}H_{36}Br_2N_6O_2$ [$M + H$] $^+$ 935.13, found 935.13.

2,7-Bis[(5-iodo-1-methyl-(pyren-1-yl)-1H-1,2,3-triazol-4-yl)-ethoxy]naphthalene 6. Copper iodide (0.030 g, 0.15 mmol) and tris[(1-benzyl-1H-1,2,3-triazol-4-yl)methyl]amine (TBTA) (0.079 g, 0.15 mmol) were stirred in dry THF (10 mL) for 20 min. The resultant solution was added to a solution of iodoalkyne **4** (0.2 g, 0.39 mmol) and 1-(azidomethyl)pyrene (0.2 g, 0.78 mmol), and the reaction was stirred in the dark for 16 h at rt before being quenched with 10% ammonium hydroxide solution (2 mL). Volatile components were removed under reduced pressure, and the resulting solid was filtered and washed with MeOH (3 \times 50 mL) to give the crude product **6** (0.14 g, 35%). Due to the extreme insolubility, the bis-iodotriazole **6** was only characterized by MS (ESI) and was used in the following step without further purification: MS (ESI) m/z calcd for $C_{52}H_{36}I_2N_6O_2$ [$M + H$] $^+$ 1031.10, found 1031.10.

2,7-Bis[(1-(pyren-1-yl)methyl-1H-1,2,3-triazol-4-yl)ethoxy]naphthalene 9. Tetrakisacetonecopper(I) hexafluorophosphate (0.09 g, 0.24 mmol) and TBTA (0.1 g, 0.19 mmol) were dissolved in dry THF (20 mL) and added to a solution of 2,7-bis(but-3-ynyloxy)naphthalene **2** (0.1 g, 0.38 mmol) and 1-(azidomethyl)pyrene (0.2 g, 0.78 mmol) in dry THF (25 mL). *N,N*-Diisopropylethylamine (0.4 mL, 1.14 mmol) was added and the reaction left to stir in the dark for 72 h at rt. The mixture was quenched with 10% ammonium hydroxide solution (2 mL), and volatile components were removed under reduced pressure; the precipitated solid was filtered and washed with MeOH (3 \times 50 mL) to give the crude product **9** (0.23 g, 37%). Due to the extreme insolubility, the bistriazole **9** was only characterized by MS (ESI) and was used in the following step without further purification: MS (ESI) m/z calcd for $C_{52}H_{38}N_6O_2$ [$M + H$] $^+$ 779.31, found 779.31.

4-(2-(2-(But-3-ynyloxy)naphthalen-7-yloxy)ethyl)-1-(pyren-1-yl)methyl-1H-1,2,3-triazole 11. Tetrakisacetonecopper(I) hexafluorophosphate (0.28 g, 0.75 mmol) and TBTA (0.4 g, 0.75 mmol)

were dissolved in dry THF (20 mL) and added to a solution of 2,7-bis(but-3-ynyloxy)naphthalene **2** (1 g, 3.79 mmol) and 1-(azidomethyl)pyrene (0.97 g, 3.79 mmol) in dry THF (25 mL). *N,N*-Diisopropylethylamine (1.31 mL, 0.75 mmol) was added, and the reaction left to stir in the dark for 48 h at room temperature. The mixture was quenched with 10% ammonium hydroxide solution (2 mL), and volatile components were removed under reduced pressure. Water (20 mL) was added, and the aqueous phase was extracted with dichloromethane (3 \times 20 mL). The combined organic fractions were dried ($MgSO_4$), filtered, and concentrated to dryness on a rotary evaporator to give a pale yellow solid. The crude product was purified by silica gel column chromatography CH_2Cl_2 /MeOH 98:2 to give a white solid (0.6 g, 30%): mp 179–180 °C; 1H NMR (300 MHz, CD_6CO) δ (ppm) 8.50 (1H, d, J = 9 Hz), 8.31–8.03 (8H, m), 7.80 (1H, s), 7.64 (1H, d, J = 9 Hz), 7.55 (1H, d, J = 9 Hz), 7.13 (1H, d, J = 3 Hz), 7.12 (1H, d, J = 3 Hz), 6.94 (1H, dd, J = 9 Hz, J = 3 Hz), 6.81 (1H, d, J = 9 Hz), 6.38 (2H, s), 4.27 (2H, t, J = 6 Hz), 4.15 (2H, t, J = 6 Hz), 3.12 (2H, t, J = 9 Hz), 2.68 (2H, td, J = 6 Hz, J = 3 Hz), 2.44 (1H, t, J = 3 Hz); ^{13}C NMR (75.5 MHz, CD_6CO) δ (ppm) 157.2, 157.0, 144.2, 136.1, 131.6, 131.2, 130.6, 129.0, 128.9, 128.8, 128.3, 127.8, 127.5, 127.2, 126.3, 125.6, 125.5, 124.9, 124.7, 124.3, 124.2, 122.6, 122.2, 116.0, 115.9, 106.2, 8.06, 70.2, 66.6, 65.8, 51.2, 25.8 18.9; MS (ESI) m/z calcd for $C_{35}H_{27}N_3O_2$ [$M + H$] $^+$ 522.21, found 522.21. Anal. Calcd for $C_{35}H_{27}N_3O_2$: C, 80.59; H, 5.22; N, 8.06. Found: C, 80.70; H, 5.15; N, 8.21.

4-(2-(2-(4-Iodobut-3-ynyloxy)naphthalen-7-yloxy)ethyl)-1-(pyren-1-yl)methyl-1H-1,2,3-triazole 12. To a solution of the alkyne **11** (0.6 g, 1.15 mmol) in acetone (20 mL) were added *N*-iodosuccinimide (0.31 g, 1.37 mmol) and catalytic amount of silver nitrate. The reaction mixture was left to stir for 24 h at room temperature in the dark under N_2 , after which a yellow suspension was formed. All volatile components were removed under reduced pressure to give a yellow oil, which was purified by silica gel column chromatography CH_2Cl_2 /MeOH 98:2 to give an off-white solid (0.4 g, 54%): mp 183–184 °C; 1H NMR (300 MHz, CD_6CO) δ (ppm) 8.50 (1H, d, J = 9 Hz), 8.32–8.02 (8H, m), 7.79 (1H, s), 7.63 (1H, d, J = 9 Hz), 7.56 (1H, d, J = 9 Hz), 7.13 (1H, d, J = 3 Hz), 7.12 (1H, d, J = 3 Hz), 6.93 (1H, dd, J = 9 Hz, J = 3 Hz), 6.81 (1H, d, J = 9 Hz), 6.35 (2H, s), 4.27 (2H, t, J = 6 Hz), 4.14 (2H, t, J = 6 Hz), 3.12 (2H, t, J = 9 Hz), 2.74 (2H, t, J = 6 Hz); ^{13}C NMR (75.5 MHz, $DMSO-d_6$) δ (ppm) 157.1, 156.8, 144.1, 136.0, 131.3, 131.1, 130.5, 129.6, 129.4, 129.3, 128.8, 128.6, 128.2, 128.0, 127.6, 126.9, 126.1, 125.9, 125.4, 124.4, 124.2, 124.1, 123.4, 123.2, 116.4, 116.2, 106.7, 90.3, 66.8, 66.1, 51.2, 25.8; MS (ESI) m/z calcd for $C_{35}H_{26}IN_3O_2$ [$M + 1$] $^+$ 648.11, found 648.11. Anal. Calcd for $C_{35}H_{26}IN_3O_2$: C, 64.92; H, 4.05; N, 6.49. Found: C, 64.81; H, 4.09; N, 6.41.

4-(2-(2-(2-(5-Iodo-1-(pyren-1-yl)methyl)-1H-1,2,3-triazol-4-yl)-ethoxy)naphthalen-7-yloxy)ethyl)-1-(pyren-1-yl)methyl-1H-1,2,3-triazole 13. Copper iodide (0.07 g, 0.37 mmol) and TBTA (0.2 g, 0.37 mmol) were stirred in dry THF (10 mL) for 20 min. The catalyst solution was added to a solution of iodoalkyne **12** (0.4 g, 0.61 mmol) and 1-(azidomethyl)pyrene (0.24 g, 0.93 mmol) and the reaction left to stir in the dark for 48 h at rt before being quenched with 10% ammonium hydroxide solution (2 mL). Volatile components were removed in vacuo, and the resulting solid was filtered and washed with MeOH (3 \times 50 mL) to give the crude product **13** (0.17 g, 32%). Due to the extreme insolubility, the bis-iodotriazole **13** was only characterized by MS (ESI) and was used in the following step without further purification: MS (ESI) m/z calcd for $C_{52}H_{37}IN_6O_2$ [$M + H$] $^+$ 905.20, found 905.20.

General Procedure for the Preparation of Receptors 7^{2+} . **2BF₄[−]**, **8²⁺·2BF₄[−]**, **10²⁺·2BF₄[−]**, and **14²⁺·2BF₄[−]**. A suspension of bistriazole **5**, **6**, **9**, or **13** (0.081 mmol) in dry dichloromethane (25 mL) was treated with trimethyloxonium tetrafluoroborate (0.18 mmol) and the reaction mixture left to stir under N_2 for 48 h at rt. Then, methanol (2 mL) was added, and all volatile components were removed under reduced pressure to give a yellow solid, which was crystallized in MeOH to give an off-white solid.

Bisbromotriazolium Receptor 7^{2+} ·2BF₄[−]. Yield 0.08 g, 87%; mp 186 °C decomposes; 1H NMR (400 MHz, CD_3CN/CD_3OD 9:1) δ (ppm) 8.27–8.05 (18H, m), 7.59 (2H, d, J = 10 Hz), 7.04 (2H, d, J = 3 Hz), 6.89 (2H, dd, J = 10 Hz, J = 3 Hz), 6.45 (4H, s), 4.30 (4H, t, J = 6 Hz), 4.26 (6H, s), 3.40 (4H, t, J = 6 Hz); ^{13}C NMR (75.5 MHz, CD_6CO) δ (ppm)

143.2, 136.7, 133.35, 132.1, 131.4, 130.5, 130.0, 129.8, 129.5, 129.2, 128.1, 127.6, 127.1, 126.9, 125.9, 125.6, 125.5, 125.0, 123.3, 118.7, 116.9, 107.1, 65.2, 55.2, 40.0, 24.9; MS (ESI) m/z calcd for $C_{54}H_{42}B_2Br_2F_8N_6O_2$ [$M^{2+} - BF_4^-$] $^+$ 1051.18, found 1051.19. Anal. Calcd for $C_{54}H_{42}B_2Br_2F_8N_6O_2$: C, 56.87; H, 3.71; N, 7.37. Found: C, 56.98; H, 3.65; N, 7.15.

Bisiodotriazolium Receptor $8^{2+} \cdot 2BF_4^-$: Yield 0.82 g, 83%; mp 182–183 °C; 1H NMR (400 MHz, CD_3CN/CD_3OD 9:1) δ (ppm) 8.27–8.10 (16H, m), 7.59 (2H, d, $J = 10$ Hz), 7.96 (2H, d, $J = 5$ Hz), 7.63 (2H, d, $J = 3$ Hz), 7.07 (2H, d, $J = 3$ Hz), 6.91 (2H, dd, $J = 10$ Hz, $J = 3$ Hz), 6.46 (4H, s), 4.32 (4H, t, $J = 6$ Hz), 4.28 (6H, s), 3.42 (4H, t, $J = 6$ Hz); ^{13}C NMR (75.5 MHz, CD_6CO) δ (ppm) 157.6, 147.6, 136.8, 133.2, 132.1, 131.5, 130.3, 130.1, 129.8, 129.5, 128.7, 128.1, 127.6, 127.1, 126.8, 125.8, 125.6, 125.5, 125.0, 123.3, 116.9, 107.2, 90.8, 65.6, 56.8, 39.8, 25.8; MS (ESI) m/z calcd for $C_{54}H_{42}B_2F_8I_2N_6O_2$ [$M^{2+} - BF_4^-$] $^+$ 1147.15, found 1147.15. Anal. Calcd for $C_{54}H_{42}B_2F_8I_2N_6O_2$: C, 52.54; H, 3.43; N, 6.81. Found: C, 52.63; H, 3.42; N, 6.69.

Bistriazolium Receptor $10^{2+} \cdot 2BF_4^-$: Yield 0.06 g, 75%; mp 167–168 °C; 1H NMR (400 MHz, CD_3CN/CD_3OD 9:1) δ (ppm) 8.29–8.08 (20H, m), 7.39 (2H, d, $J = 10$ Hz), 6.92 (2H, d, $J = 3$ Hz), 6.68 (2H, dd, $J = 9$ Hz, $J = 3$ Hz), 6.42 (4H, s), 4.21 (6H, s), 4.20 (4H, t, $J = 6$ Hz), 3.24 (4H, t, $J = 6$ Hz); ^{13}C NMR (75.5 MHz, $DMSO-d_6$) δ (ppm) 156.8, 142.3, 135.8, 131.1, 130.5, 129.6, 129.5, 129.4, 129.2, 128.9, 127.6, 127.2, 126.6, 126.4, 126.2, 125.6, 124.5, 124.0, 122.9, 116.4, 106.9, 64.7, 54.5, 38.4, 23.7; MS (ESI) m/z calcd for $C_{54}H_{44}B_2F_8N_6O_2$ [$M^{2+} - BF_4^-$] $^+$ 895.35, found 895.35. Anal. Calcd for $C_{54}H_{44}B_2F_8N_6O_2$: C, 66.01; H, 4.51; N, 8.55. Found: C, 66.12; H, 4.42; N, 8.59.

Mixed Halogen- and Hydrogen-Bonding Receptor $14^{2+} \cdot 2BF_4^-$: Yield 0.029 g, 32%; mp 179–180 °C; 1H NMR (400 MHz, CD_3CN/CD_3OD 9:1) δ (ppm) 8.15–8.07 (19H, m), 7.96 (1H, d, $J = 10$ Hz), 7.57 (1H, d, $J = 10$ Hz), 8.43 (1H, d, $J = 10$ Hz), 7.00 (1H, d, $J = 3$ Hz), 6.98 (1H, d, $J = 3$ Hz), 6.90 (1H, dd, $J = 10$ Hz, $J = 3$ Hz), 6.68 (1H, dd, $J = 10$ Hz, $J = 3$ Hz), 6.45 (2H, s), 6.44 (2H, s), 4.29 (2H, t, $J = 6$ Hz), 4.28 (3H, s), 4.24 (2H, t, $J = 6$ Hz), 4.22 (3H, s), 3.42 (2H, t, $J = 6$ Hz), 3.26 (2H, t, $J = 9$ Hz); ^{13}C NMR (75.5 MHz, CD_6CO) δ (ppm) 157.7, 156.9, 147.7, 147.6, 136.8, 136.7, 133.3, 133.2, 132.1, 132.0, 131.5, 131.4, 130.3, 130.2, 130.1, 130.1, 129.8, 128.7, 129.5, 129.4, 128.8, 128.6, 128.1, 128.0, 127.7, 127.6, 127.3, 127.2, 126.9, 126.8, 125.8, 125.7, 125.6, 125.5, 125.4, 125.0, 124.9, 124.8, 123.3, 123.2, 116.5, 107.3, 107.0, 90.8, 90.5, 65.6, 65.4, 56.9, 56.7, 40.0, 39.8, 25.8, 25.5; MS (ESI) m/z calcd for $C_{54}H_{43}B_2F_8IN_6O_2$ [$M^{2+} - BF_4^-$] $^+$ 1021.25, found 1021.25. Anal. Calcd for $C_{54}H_{43}B_2F_8IN_6O_2$: C, 58.51; H, 3.91; N, 7.58. Found: C, 58.63; H, 3.85; N, 7.69.

■ ASSOCIATED CONTENT

■ Supporting Information

1H and ^{13}C NMR spectra, Job plot experiments, ^{31}P NMR fluorescence and UV–vis anion binding studies, optimized geometry of the receptors and complexes. This material is available free of charge via the Internet at <http://pubs.acs.org>.

■ AUTHOR INFORMATION

Corresponding Authors

*E-mail: antocaba@um.es.

*E-mail: pmolina@um.es.

*E-mail: ibon@iqm.csic.es.

Notes

The authors declare no competing financial interest.

■ ACKNOWLEDGMENTS

This work was supported by European Commission FP7-PEOPLE-2012-CIG No. 321716 and MICINN-Spain and FEDER, project CTQ2011-27175, CTQ2013-46096-P, Fundación Séneca (CARM) Project 04509/GERM/06. Thanks are also given to the Ministerio de Economía y Competitividad of Spain (Project CTQ2012-13129-C02-02) and the Comunidad Autónoma de Madrid (Project MADRISOLAR2, ref S2009/

PPQ-1533). A.C. acknowledges Ministerio de Ciencia e Innovación of Spain for funding his work through a contract of the Ramón y Cajal Program. F.Z. acknowledges Ministerio de Economía y Competitividad of Spain for a contract of the Subprogram Juan de la Cierva, 2012.

■ REFERENCES

- (1) (a) Beer, P. D.; Gale, P. A. *Angew. Chem., Int. Ed.* **2001**, *40*, 486–512. (b) O’Neil, E. J.; Smith, B. D. *Coord. Chem. Rev.* **2006**, *250*, 3068–3080. (c) Sessler, J. L.; Gale, P. A.; Cho, W.-S. *Anion Receptor Chemistry*; RSC: Cambridge, 2006. (d) Llinares, J. M.; Powell, D.; Bowman-James, K. *Coord. Chem. Rev.* **2003**, *240*, 57–75. (e) Martínez-Máñez, R.; Sancenón, F. *Coord. Chem. Rev.* **2006**, *250*, 3081–3093. (f) Gunnlaugsson, T.; Glynn, M.; Tocci, G. M.; Kruger, P. E.; Pfeffer, F. M. *Coord. Chem. Rev.* **2006**, *250*, 3094–3117. (g) Rice, C. R. *Coord. Chem. Rev.* **2006**, *250*, 3190. (h) Gale, P. A.; García-Garrido, S. E.; Garric, J. *Chem. Soc. Rev.* **2008**, *37*, 151–190. (i) Pérez, J.; Riera, L. *Chem. Soc. Rev.* **2008**, *37*, 2658–2667. (j) Steed, J. W. *Chem. Soc. Rev.* **2009**, *38*, 506–519. (k) Kubik, S. *Chem. Soc. Rev.* **2009**, *38*, 585–605. (l) Hua, Y.; Flood, A. H. *Chem. Soc. Rev.* **2010**, *39*, 1262–1271.
- (2) (a) Quiñonero, D.; Garau, C.; Frontera, A.; Ballester, P.; Costa, A.; Deyá, P. M. *Angew. Chem., Int. Ed.* **2002**, *41*, 3389–3392. (b) Alkorta, I.; Elguero, J. *J. Am. Chem. Soc.* **2002**, *124*, 8593–8598. (c) Mascal, M. *Angew. Chem., Int. Ed.* **2006**, *45*, 2890–2893. (d) Mascal, M.; Yakovlev, I.; Nikitin, E. B.; Fettingner, J. C. *Angew. Chem., Int. Ed.* **2007**, *46*, 8782–8784. (e) Hay, B. P.; Bryantsev, V. S. *Chem. Commun.* **2008**, 2417–2428. (f) Schottel, B. L.; Chifotides, H. T.; Dunbar, K. R. *Chem. Soc. Rev.* **2008**, *37*, 68–83. (g) Barryman, O. B.; Johnson, D. W. *Chem. Commun.* **2009**, 3143–3153. (h) Ni, X.-L.; Zeng, N.; Redshaw, C.; Yamato, T. *J. Org. Chem.* **2011**, *76*, 5696–5702.
- (3) (a) Metrangolo, P.; Neukirch, H.; Pilati, T.; Resnati, G. *Acc. Chem. Res.* **2005**, *38*, 386–395. (b) Politzar, P.; Lane, P.; Concha, M. C.; Ma, Y.; Murray, J. S. *J. Mol. Modell.* **2007**, *23*, 305–311. (c) Metrangolo, P.; Meyer, F.; Pilati, T.; Resnati, G.; Terraneo, G. *Angew. Chem., Int. Ed.* **2008**, *47*, 6114–6127. (d) Erdélyi, M. *Chem. Soc. Rev.* **2012**, *41*, 3547–3557. (e) Beale, T. M.; Chudzinski, M. G.; Sarwar, M. G.; Taylor, M. S. *Chem. Soc. Rev.* **2013**, *42*, 1667–1680.
- (4) Metrangolo, P.; Resnati, G. *Science* **2008**, *321*, 918–919.
- (5) (a) Caronna, T.; Liantonio, R.; Logothetis, T. A.; Metrangolo, P.; Pilati, T.; Resnati, G. *J. Am. Chem. Soc.* **2004**, *126*, 4500–4501. (b) Sun, A.; Goroff, N. S.; Lauther, J. W. *Science* **2006**, *312*, 1030–1034. (c) Rissanen, K. *CrystEngComm* **2008**, *10*, 1107–1113. (d) Carvallo, G.; Metrangolo, P.; Pilati, T.; Resnati, G.; Sansotera, M.; Terraneo, G. *Chem. Soc. Rev.* **2010**, *39*, 3772–3783.
- (6) Metrangolo, P.; Carcenac, Y.; Lahtinen, M.; Pilati, T.; Rissanen, K.; Vij, A.; Resnati, G. *Science* **2009**, *323*, 1461–1464.
- (7) Fourmigué, M.; Batail, P. *Chem. Rev.* **2004**, *104*, 5379–5418.
- (8) (a) Nguyen, H. L.; Horton, P. N.; Hursthouse, M. B.; Legon, A. C.; Bruce, D. W. *J. Am. Chem. Soc.* **2004**, *126*, 16–17. (b) Metrangolo, P.; Prasang, C.; Resnati, G.; Liantonio, R.; Whitwood, A. C.; Bruce, C. *Commun. Chem.* **2006**, 3290–3292. (c) Cincic, D.; Friscic, T.; Jones, W. *Chem.—Eur. J.* **2008**, *14*, 747–753. (d) Metrangolo, P.; Meyer, F.; Pilati, T.; Proserpio, D. M.; Resnati, G. *Cryst. Growth Des.* **2008**, *8*, 654–659. (e) Xu, J. W.; Liu, X. M.; Ng, J. K. P.; Lin, T. T.; He, C. B. *J. Mater. Chem.* **2006**, *16*, 3540–3595. (f) Bruce, D. W.; Metrangolo, P.; Meyer, F.; Prasang, C.; Resnati, G.; Terraneo, G.; A. C. Whitwood, A. C. *New J. Chem.* **2008**, *32*, 477–482. (g) Zordan, F.; Brammer, L.; Sherwood, P. J. *Am. Chem. Soc.* **2005**, *127*, 5979–5989. (h) Liantonio, L.; Metrangolo, P.; Meyer, F.; Pilati, T.; Navarrini, W.; Resnati, G. *Chem. Commun.* **2006**, 1819–1821. (i) Graeme, R. H.; Paul, J.; John, M.; Llew, R.; Aaron, S. M. *Chem.—Eur. J.* **2009**, *15*, 4156–4164. (j) Prasang, C.; Nguyen, H. L.; Horton, P. N.; Whitwood, A. C.; Bruce, D. W. *Chem. Commun.* **2008**, 6164–6166.
- (9) (a) Dimitrijevic, E.; Kvak, O.; Taylor, M. S. *Chem. Commun.* **2010**, 46, 9025–9027. (b) Sarwar, M. G.; Dragisic, B.; Dimitrijevic, E.; Taylor, M. S. *Chem.—Eur. J.* **2013**, *19*, 2050–2058. (c) Mele, A.; Metrangolo, P.; Neukirch, H.; Pilati, T.; Resnati, G. *J. Am. Chem. Soc.* **2005**, *127*, 14972–14973.

- (10) Sarwar, M. G.; Dragisic, B.; Sagoo, S.; Taylor, M. S. *Angew. Chem., Int. Ed.* **2010**, *49*, 1674–1677.
- (11) Chudzinski, M. G.; McClary, C. A.; Taylor, M. S. *J. Am. Chem. Soc.* **2011**, *133*, 10559.
- (12) (a) Caballero, A.; White, N. G.; Beer, P. D. *Angew. Chem., Int. Ed.* **2011**, *50*, 1845–1848. (b) Khilah, N. L.; Wise, M. D.; Beer, P. D. *Cryst. Growth. Des.* **2011**, *11*, 4565–4571. (c) Walter, S. M.; Kneip, F.; Rout, L.; Schmidtchen, F. P.; Herdtweck, E.; Huber, S. M. *J. Am. Chem. Soc.* **2012**, *134*, 8507–8512. (d) Zapata, F.; Caballero, A.; White, N. G.; Claridge, T. D. W.; Costa, P. J.; Felix, V.; Beer, P. D. *J. Am. Chem. Soc.* **2012**, *134*, 11533–11541.
- (13) Khilah, N. L.; Wise, M. D.; Serpell, C. J.; Thompson, A. L.; White, N. G.; Christensen, K. E.; Beer, P. D. *J. Am. Chem. Soc.* **2010**, *132*, 11893–11895.
- (14) (a) Cametti, M.; Raatikainen, K.; Metrangolo, P.; Pilati, T.; Terraneo, G.; Resnati, G. *Org. Biomol. Chem.* **2012**, *10*, 1329–1333. (b) Gilday, L. C.; White, N. G.; Beer, P. D. *Dalton Trans.* **2013**, *42*, 15766–15773.
- (15) Mitsunobu, O. *Synthesis* **1981**, *1*, 1–28.
- (16) Hein, J. E.; Tripp, J. C.; Krasnova, L. B.; Sharpless, K. B.; Fokin, V. *Angew. Chem., Int. Ed.* **2009**, *48*, 8018–8021.
- (17) Park, S. Y.; Yoon, J. H.; Hong, C. S.; Souane, R.; Kim, J. S.; Matthews, S. E.; Vicens, J. J. *Org. Chem.* **2008**, *73*, 8212–8218.
- (18) Winnick, F. M. *Chem. Rev.* **1993**, *93*, 587–614.
- (19) (a) Basu, G.; Kubasik, M.; Anglos, D.; Secor, B.; Kuki, A. *J. Am. Chem. Soc.* **1990**, *112*, 9410–9411. (b) Solovyov, K. N.; Borisevich, E. A. *Phys.-Usp.* **2005**, *48*, 231. (c) Rae, M.; Perez-Balderas, F.; Baleizao, C.; Fedorov, A.; Cavaleiro, J. A. S.; Tomé, A. C.; Berberan-Santos, M. N. *J. Phys. Chem. B* **2006**, *110*, 12809–12814.
- (20) Specfit/32 Global Analysis System, 1999–2004 Spectrum Software Associates (SpecSoft@compuserve.com). The Specfit program was acquired from Bio-logic, SA (www.bio-logic.info) in January 2005. The equation to be adjusted by nonlinear regression, using the above mentioned software was $\Delta A/b = \{K_{11}\Delta\epsilon_{HG}[H]_{\text{tot}}[G]\}/\{1 + K_{11}[G]\}$, where H = host, G = guest, HG = complex, ΔA = variation in the absorption, b = cell width, K_{11} = association constant for a 1:1 model, and $\Delta\epsilon_{HG}$ = variation of molar absorptivity.
- (21) (a) Lipscombe, W. N.; Sträter, N. *Chem. Rev.* **1996**, *96*, 2375–2433. (b) Tabary, T.; Lu, J. J. *Immunol. Methods* **1992**, *156*, 55. (c) Nyren, P. *Anal. Biochem.* **1987**, *167*, 235–238.
- (22) Xu, S.; He, M.; Yu, H.; Cai, X.; Tan, X.; Lu, B.; Shu, B. *Anal. Biochem.* **2001**, *299*, 188–193.
- (23) (a) Doherty, M.; Becher, C.; Regan, M.; Jones, A.; Ledingham, J. *Ann. Rheum. Dis.* **1996**, *55*, 432–436. (b) Timms, A. E.; Zhang, Y.; Russell, R. G.; Brown, M. A. *Rheumatology* **2002**, *41*, 725–729.
- (24) Sánchez, G.; Curiel, D.; Tatkiecz, W.; Ratera, I.; Tarraga, A.; Veciana, J.; Molina, P. *Chem. Sci.* **2014**, *5*, 2328–2335.
- (25) Caballero, A.; Zapata, F.; González, L.; Molina, P.; Alkorta, I.; Elguero, J. *Chem. Commun.* **2014**, *50*, 4680–4682.
- (26) Hynes, M. J. *J. Chem. Soc., Dalton Trans.* **1993**, 311–312.
- (27) ADF2013, SCM, Theoretical Chemistry, Vrije Universiteit, Amsterdam, The Netherlands, <http://www.scm.com>.
- (28) (a) Pye, C. C.; Ziegler, T. *Theor. Chem. Acc.* **1999**, *101*, 396–408. (b) Klamt, A.; Schüürmann, G. *J. Chem. Soc., Perkin Trans. 2* **1993**, 799–805. (c) Klamt, A. *J. Phys. Chem.* **1995**, *55*, 2224–2235. (d) Klamt, A.; Jones, V. J. *Chem. Phys.* **1996**, *105*, 9972–9981.
- (29) Gonzalez, C.; Lim, E. C. *J. Phys. Chem. A* **2003**, *107*, 10105–10110.
- (30) Grimme, S. *J. Comput. Chem.* **2004**, *25*, 1463–1473.
- (31) (a) Perdew, J. P.; Burke, K.; Ernzerhof, M. *Phys. Rev. Lett.* **1996**, *77*, 3865–3868. (b) Grimme, S. *J. Comput. Chem.* **2006**, *27*, 1787–1799. (c) van Lenthe, E.; Baerends, E. J. *J. Comput. Chem.* **2003**, *24*, 1142–1156.
- (32) *The Nature of the Hydrogen Bond: Outline of a Comprehensive Hydrogen Bond Theory*; Gilli, G.; Gilli, P., Eds.; Oxford University Press: New York, 2009.
- (33) Gilli, P.; Pretto, L.; Bertolasi, V.; Gilli, G. *Acc. Chem. Res.* **2009**, *42*, 33–44.
- (34) *Halogen Bonding: Fundamentals and Applications*; Metrangolo, P.; Resnati, G., Eds.; Springer: Berlin, 2008.
- (35) Sarwar, M. G.; Dragisic, B.; Salsberg, L. J.; Gouliaras, C.; Taylor, M. S. *J. Am. Chem. Soc.* **2010**, *132*, 1646–1653.
- (36) *Supramolecular Chemistry of Anions*; Bianchi, A.; Bowman-James, K.; García-España, E., Eds.; Wiley-VCH: New York, 1997; p 227.
- (37) Reichardt, C. *Solvents and Solvent Effects in Organic Chemistry*, 3rd ed. Updated and Enlarged; Wiley-VCH: Weinheim, Germany, 2003; p 140.
- (38) Schneider, H. J.; Mohammad-Ali, A. K. Receptors for Organic Guest Molecules: General Principles. In *Comprehensive Supramolecular Chemistry*; Atwood, J. L., Davies, J. E. D., MacNicol, D. D., Vögtle, F., Eds.; Pergamon: Oxford, 1996; Vol. 2, p 75.
- (39) Smithrud, D. B.; Sanford, E. M.; Chao, I.; Ferguson, S. B.; Carcanague, D. R.; Evanseck, J. D.; Houk, K. N.; Diederich, F. *Pure Appl. Chem.* **1990**, *62*, 2227–2236.